

Coherent Distributed Array Imaging under Unknown Position Perturbations

Liu, D.; Kamilov, U.; Boufounos, P.T.

TR2016-092 September 2016

Abstract

We consider a distributed array imaging problem for detecting targets in a region of interest (ROI), where the radar sensors are perturbed with location errors corresponding to several wavelengths. In order to improve the imaging performance, we propose a method based on compressive sensing that can simultaneously compensate for position-induced phase errors and perform focused imaging. Compared to existing autofocusing methods that typically exhibit poor performance for large position errors, our method can form sharp images of targets situated in the ROI even for position errors that are ten wavelengths large. We validate our method on simulated noisy data.

International Workshop on Compressed Sensing Theory and its Applications to Radar, Sonar, and Remote Sensing (CoSeRa)

This work may not be copied or reproduced in whole or in part for any commercial purpose. Permission to copy in whole or in part without payment of fee is granted for nonprofit educational and research purposes provided that all such whole or partial copies include the following: a notice that such copying is by permission of Mitsubishi Electric Research Laboratories, Inc.; an acknowledgment of the authors and individual contributions to the work; and all applicable portions of the copyright notice. Copying, reproduction, or republishing for any other purpose shall require a license with payment of fee to Mitsubishi Electric Research Laboratories, Inc. All rights reserved.

Coherent Distributed Array Imaging under Unknown Position Perturbations

Dehong Liu, Ulugbek S. Kamilov, and Petros T. Boufounos
Mitsubishi Electric Research Laboratories (MERL)
201 Broadway, Cambridge, MA 02139
Email: {liudh, kamilov, petrosb}@merl.com

Abstract—We consider a distributed array imaging problem for detecting targets in a region of interest (ROI), where the radar sensors are perturbed with location errors corresponding to several wavelengths. In order to improve the imaging performance, we propose a method based on compressive sensing that can simultaneously compensate for position-induced phase errors and perform focused imaging. Compared to existing autofocusing methods that typically exhibit poor performance for large position errors, our method can form sharp images of targets situated in the ROI even for position errors that are ten wavelengths large. We validate our method on simulated noisy data.

Keywords—Coherent radar imaging, distributed sensing, autofocus, compressive sensing

I. INTRODUCTION

The resolution of radar images depends on the size of aperture formed by the sensor array. In order to form a large physical aperture one appealing option is to employ several small-aperture arrays distributed in space. Typically, spatial distribution of such arrays is not uniform; however, by processing the data collaboratively, they can still form a large effective aperture. It has been shown that, when the locations of arrays are precisely known and the received signals are synchronized, such a distributed sensing scheme can significantly improve the imaging resolution [1]. Additionally, it was recently shown that compressive sensing (CS) based techniques and sparsity-constraints can further reduce ghost targets in the image due to non-uniformity of array locations [2]. Distributed array imaging schemes also exhibit several other practical benefits such as flexibility of platform placement, low operation and maintenance costs, and robustness to individual sensor failures.

One of the practical challenges in distributed array imaging is that the locations of the arrays are only known approximately due to various position perturbations. Such perturbations can be as large as several wavelengths of the radar's central frequency. Although modern navigation systems such as Global Positioning System (GPS) can measure positions with a relatively high accuracy, the range of resulting errors is still beyond the requirements of high-resolution radar imaging. For position perturbations that are larger than one wavelength, the phase wrapping in the measured signal complicates coherent imaging. Incoherent processing, on the other hand, inevitably degrades the imaging resolution and leads to loss of focus in the resulting image. Therefore, there is a need for an imaging method for distributed arrays that can perform autofocusing in order to compensate for the unknown position perturbations.

There exist several autofocusing methods for imaging using

a single sensor array, which are realized by compensating either for the phase or the position errors [3]–[8]. In recent years, the emergence of CS-based radar imaging has resulted in several new methods that do autofocusing by incorporating sparsity constraints into image formation [8]–[11]. When position errors are significantly smaller than the central wavelength, CS-based autofocusing algorithms formulate imaging as a non-linear optimization problem with a perturbed projection matrix. However, error bounds in the solution depend on position errors [12], [13]. When position errors are greater than the central wavelength, a CS-based method with data coherence analysis was shown to perform autofocused imaging [11].

In this paper, we propose an autofocusing method for distributed arrays perturbed with unknown positions errors. The proposed method extends our previous work on coherent distributed radar imaging [2] by allowing location ambiguities, and on autofocusing for a single sensor array [11] by investigating distributed sensing with multiple sensors. In particular, we consider a multi-static radar imaging problem where one transmitting/receiving radar platform and multiple receiving radar platforms are moving towards a region of interest (ROI) with position perturbations. The objective is to detect targets inside the ROI. Due to inaccurate positioning and motion errors, the actual array positions are perturbed up to several times the central radar wavelength. Although the image resolution of each sensor array is low due to its small aperture size, a high-resolution image can be formed by jointly processing the outputs of all distributed arrays with well-compensated position errors. Our approach is based on an assumption of a sparse scene, and is realized iteratively by solving series of optimization problems for compensating position-induced phase errors, exploiting target signatures, and estimating antenna positions. Compared to existing approaches, our method substantially improves imaging performance, even for position perturbations that are up to ten times the central wavelength, thus yielding a sharp image for targets located in the ROI.

This paper is organized as follows. In Section II, we build a general data acquisition model for distributed sensor arrays with position perturbations. In Section III, we describe the details of our autofocusing distributed array imaging method with data coherence analysis and group sparsity constraints. Imaging results with simulated noisy data are presented in Section IV with conclusion in Section V.

II. DATA ACQUISITION MODEL

We consider a two-dimensional (2D) radar imaging problem in which a total of D distributed radar platforms are

moving towards a ROI to detect targets within. Each platform forms a forward-looking virtual array. We use $p(t)$ and $P(\omega)$ to denote the time-domain source pulse and its corresponding frequency spectrum, respectively, where

$$P(\omega) = \int_{\mathbb{R}} p(t)e^{-j\omega t} dt. \quad (1)$$

The scattered field at location \mathbf{r}' due to the target with a phase center at \mathbf{l} and the excitation pulse originating from \mathbf{r} , can be approximated with the first-Born approximation as [14]

$$Y_I(\omega, \mathbf{r}, \mathbf{r}') = P(\omega)S(\omega, \mathbf{l})G(\omega, \mathbf{l}, \mathbf{r})G(\omega, \mathbf{r}', \mathbf{l}), \quad (2)$$

where $S(\omega, \mathbf{l})$ is a complex-valued function of frequency, which accounts for all the terms due to the asymptotic approximation; $G(\omega, \mathbf{l}, \mathbf{r})$ accounts for propagation from \mathbf{r} to \mathbf{l} and can be represented by

$$G(\omega, \mathbf{l}, \mathbf{r}) = a(\mathbf{r}, \mathbf{l})e^{-j\omega \frac{\|\mathbf{r}-\mathbf{l}\|}{c}}, \quad (3)$$

where $a(\mathbf{r}, \mathbf{l})$ represents the overall magnitude attenuation due to the antenna beampattern and the propagation between \mathbf{r} and \mathbf{l} , and $e^{-j\omega \frac{\|\mathbf{r}-\mathbf{l}\|}{c}}$ is the phase change term of the received signal relative to the source pulse after propagating distance $\|\mathbf{r} - \mathbf{l}\|$ at speed c . For simplicity, we have omitted the noise term from eq. (2).

Without a loss of generality, we assume that there are up to K targets, each with a phase center located at a pixel in the ROI image. Let $i_k \in \{1, \dots, I\}$ be the pixel index of the k th target and \mathbf{l}_{i_k} be the corresponding location. Let $\mathbf{r}_{d,n}$ be the ideal location of the n th virtual element of the d th array, where $n \in \{1, 2, \dots, N\}$ and $d \in \{1, 2, \dots, D\}$. Due to position perturbations, the actual measurements are taken at $\tilde{\mathbf{r}}_{d,n} = \mathbf{r}_{d,n} + \boldsymbol{\varepsilon}_{d,n}$, where $\boldsymbol{\varepsilon}_{d,n}$ stands for corresponding unknown position perturbation with $0 \leq |\boldsymbol{\varepsilon}_{d,n}| \leq 10\lambda$, and λ is the wavelength of the radar central frequency. The overall signal received by the perturbed array is then a superposition of scattered waves from all targets in the ROI. For the source signal transmitted by the n th virtual element of the d_0 th platform, where $d_0 \in \{1, 2, \dots, D\}$, we consider measurements by the n th virtual element of the d th platform at a discrete frequency ω_m , where $m = 1, 2, \dots, M$. After range compression, we end up with an $M \times D \times N$ data cube $\tilde{\mathbf{Y}}$, whose entry (m, d, n) is

$$\tilde{\mathbf{Y}}(m, d, n) = \sum_{k=1}^K |P(\omega_m)|^2 S(\omega_m, \mathbf{l}_{i_k}) a(\tilde{\mathbf{r}}_{d_0,n}, \mathbf{l}_{i_k}) a(\tilde{\mathbf{r}}_{d,n}, \mathbf{l}_{i_k}) \exp\left(-j\omega_m \frac{\|\tilde{\mathbf{r}}_{d_0,n} - \mathbf{l}_{i_k}\| + \|\tilde{\mathbf{r}}_{d,n} - \mathbf{l}_{i_k}\|}{c}\right). \quad (4)$$

To simplify notation, we define a scalar

$$x_{i_k}^{(d,n)} = a(\tilde{\mathbf{r}}_{d_0,n}, \mathbf{l}_{i_k}) a(\tilde{\mathbf{r}}_{d,n}, \mathbf{l}_{i_k}) \sum_{m=1}^M |P^2(\omega_m) S(\omega_m, \mathbf{l}_{i_k})|^2, \quad (5)$$

an $M \times 1$ unit vector

$$\phi_{i_k} = \begin{bmatrix} \frac{|P(\omega_1)|^2 S(\omega_1, \mathbf{l}_{i_k})}{\sum_{m=1}^M |P^2(\omega_m) S(\omega_m, \mathbf{l}_{i_k})|^2} \\ \frac{|P(\omega_2)|^2 S(\omega_2, \mathbf{l}_{i_k})}{\sum_{m=1}^M |P^2(\omega_m) S(\omega_m, \mathbf{l}_{i_k})|^2} \\ \vdots \\ \frac{|P(\omega_M)|^2 S(\omega_M, \mathbf{l}_{i_k})}{\sum_{m=1}^M |P^2(\omega_m) S(\omega_m, \mathbf{l}_{i_k})|^2} \end{bmatrix}, \quad (6)$$

and an $M \times 1$ exponential vector

$$\tilde{\boldsymbol{\psi}}_{i_k}^{(d,n)} = \begin{bmatrix} e^{-j\omega_1 \frac{\|\tilde{\mathbf{r}}_{d_0,n} - \mathbf{l}_{i_k}\| + \|\tilde{\mathbf{r}}_{d,n} - \mathbf{l}_{i_k}\|}{c}} \\ e^{-j\omega_2 \frac{\|\tilde{\mathbf{r}}_{d_0,n} - \mathbf{l}_{i_k}\| + \|\tilde{\mathbf{r}}_{d,n} - \mathbf{l}_{i_k}\|}{c}} \\ \vdots \\ e^{-j\omega_M \frac{\|\tilde{\mathbf{r}}_{d_0,n} - \mathbf{l}_{i_k}\| + \|\tilde{\mathbf{r}}_{d,n} - \mathbf{l}_{i_k}\|}{c}} \end{bmatrix}. \quad (7)$$

The vector $\tilde{\mathbf{y}}^{(d,n)} = \tilde{\mathbf{Y}}(:, d, n)$ can then be written in a matrix-vector form as

$$\begin{aligned} \tilde{\mathbf{y}}^{(d,n)} &= \sum_{k=1}^K (\phi_{i_k} \circ \tilde{\boldsymbol{\psi}}_{i_k}^{(d,n)}) x_{i_k}^{(d,n)} \\ &= [\Phi \circ \tilde{\Psi}^{(d,n)}] \mathbf{x}^{(d,n)} = \tilde{\Gamma}^{(d,n)} \mathbf{x}^{(d,n)}, \end{aligned} \quad (8)$$

where the symbol \circ represents element-wise product. Here, $\tilde{\Gamma}^{(d,n)} = [\phi_1 \circ \tilde{\boldsymbol{\psi}}_1^{(d,n)}, \dots, \phi_I \circ \tilde{\boldsymbol{\psi}}_I^{(d,n)}]$ is an $M \times I$ projection matrix of the n th antenna position in the d th array, $\mathbf{x}^{(d,n)} = [x_1^{(d,n)}, \dots, x_I^{(d,n)}]^T$ is a K -sparse vector of target scattering coefficients. It is important to note that ϕ_{i_k} is a target signature vector independent of antenna positions, which is extracted from measured data efficiently during the imaging formation.

III. IMAGING WITH AUTOFOCUS

A. Optimization problem

Since the antenna positions $\tilde{\mathbf{r}}_{d,n}$ are not known exactly, image formation that treats the perturbed array as a uniform array generally yields a de-focused image with its quality related to the position perturbations. In order to perform imaging with autofocus, we solve the following sparsity constrained optimization problem

$$\begin{aligned} \min_{\tilde{\Gamma}, \mathbf{x}} & \left\{ \sum_{d=1}^D \sum_{n=1}^N \|\tilde{\mathbf{y}}^{(d,n)} - \tilde{\Gamma}^{(d,n)} \mathbf{x}^{(d,n)}\|_2^2 \right\} \\ \text{subject to} & \left\| \sum_{d=1}^D \sum_{n=1}^N \mathbf{x}^{(d,n)} \right\|_0 \leq K, \end{aligned} \quad (9)$$

where $\tilde{\Gamma} = \{\tilde{\Gamma}^{(d,n)}\}_{d,n}$ and $\mathbf{x} = \{\mathbf{x}^{(d,n)}\}_{d,n}$. The above optimization problem is similar to the group sparsity formulation that is often used in CS imaging [15]. Specifically, it relies on the fact that all unknown vectors share the same non-zero support but have generally different values within the support. However, the autofocusing problem formulated in eq. (9) is more general than the group sparsity problem since the projection matrices are not identical across all antennas. They share the same target signature vector ϕ_{i_k} , but are different in the unknown exponential term $\tilde{\boldsymbol{\psi}}_{i_k}^{(d,n)}$. Motivated by the orthogonal matching pursuit algorithm, we solve (9) iteratively with maximum of K iterations. At the k th iteration, given the residual data $\tilde{\mathbf{y}}_{\text{res},k}^{(d,n)}$, which is initialized as measured data, and updated at each iteration by removing the signals of all the detected targets, we have a degenerated problem

$$\begin{aligned} \min_{\tilde{\Gamma}, \mathbf{x}} & \left\{ \sum_{d=1}^D \sum_{n=1}^N \|\tilde{\mathbf{y}}_{\text{res},k}^{(d,n)} - \tilde{\Gamma}^{(d,n)} \mathbf{x}^{(d,n)}\|_2^2 \right\} \\ \text{subject to} & \left\| \sum_{d=1}^D \sum_{n=1}^N \mathbf{x}^{(d,n)} \right\|_0 = 1. \end{aligned} \quad (10)$$

Note that the ℓ_0 -norm of vectors $\{\mathbf{x}^{(d,n)}\}$ is 1, where the only non-zero component corresponding the k th strongest target phase center. Let the image reconstructed by the residual data $\tilde{\mathbf{Y}}_{\text{res},k}^{(d,n)}$ be $\hat{\mathbf{x}}_{\text{res},k}$. A target is then detected at location \mathbf{l}_{i_k} where the maximum absolute value of $\hat{\mathbf{x}}_{\text{res},k}$ is observed as follows

$$i_k = \arg \max_i \{ |\hat{\mathbf{x}}_{\text{res},k}(i)| \}. \quad (11)$$

To determine $\tilde{\Gamma}$, we stack $\{\tilde{\mathbf{y}}_{\text{res},k}^{(d,n)}\}$ to form an $M \times ND$ matrix

$$\tilde{\mathbf{Y}}_{\text{res},k} = [\tilde{\mathbf{y}}_{\text{res},k}^{(1,1)}, \tilde{\mathbf{y}}_{\text{res},k}^{(1,2)}, \dots, \tilde{\mathbf{y}}_{\text{res},k}^{(D,1)}, \dots, \tilde{\mathbf{y}}_{\text{res},k}^{(D,N)}]. \quad (12)$$

Similarly, vectors $\{\tilde{\Gamma}^{(d,n)} \mathbf{x}^{(d,n)}\}$ were also stacked into an $M \times ND$ matrix. The stacked matrix $[\tilde{\Gamma}^{(d,n)} \mathbf{x}^{(d,n)}]$ is then re-organized as

$$\begin{aligned} & [\tilde{\Gamma}^{(1,1)} \mathbf{x}^{(1,1)}, \tilde{\Gamma}^{(1,2)} \mathbf{x}^{(1,2)}, \dots, \tilde{\Gamma}^{(D,N)} \mathbf{x}^{(D,N)}] \\ & = [x_{i_k}^{(1,1)} \phi_{i_k}, \dots, x_{i_k}^{(D,N)} \phi_{i_k}] \circ [\tilde{\psi}_{i_k}^{(1,1)}, \dots, \tilde{\psi}_{i_k}^{(D,N)}] \\ & = \mathbf{E}_{i_k} \circ \tilde{\Psi}_{i_k}, \end{aligned} \quad (13)$$

where $\mathbf{E}_{i_k} = [x_{i_k}^{(1,1)} \cdot \phi_{i_k}, \dots, x_{i_k}^{(D,N)} \cdot \phi_{i_k}]$ is an $M \times DN$ rank-one matrix, whose dominant left singular vector is exactly ϕ_{i_k} , and $\tilde{\Psi}_{i_k} = [\tilde{\psi}_{i_k}^{(1,1)}, \dots, \tilde{\psi}_{i_k}^{(D,N)}]$ is an $M \times DN$ exponential matrix parameterized by the distance between the k th target and the perturbed distributed arrays. Based on (12) and (13), and given \mathbf{x} , $\tilde{\Gamma}$ can be determined by solving

$$\min_{\mathbf{E}_{i_k}, \tilde{\Psi}_{i_k}} \|\tilde{\mathbf{Y}}_{\text{res},k} - \mathbf{E}_{i_k} \circ \tilde{\Psi}_{i_k}\|_{\text{F}}^2, \quad \text{s.t. } \text{rank}(\mathbf{E}_{i_k}) = 1, \quad (14)$$

where the subscript F represents the Frobenius norm of the matrix. Equation (14) is then solved by an inner loop in which we alternately update $\tilde{\Psi}_{i_k}$ by data coherence analysis, described in Section III-B, and \mathbf{E}_{i_k} by dominant target signature analysis, as described in Section III-C.

B. Data coherence analysis

To estimate time lags, we use the cross-correlation (CC) of signals. Specifically, given $\tilde{\mathbf{Y}}_{\text{res},k}$ and \mathbf{E}_{i_k} , we compute the time-delay parameter $\tilde{\Psi}_{i_k}$ by finding the delay corresponding to the maximum of the CC function. However, CC is not concave and, thus, may have multiple local maxima. To reduce ambiguity in the CC function, we extract the k th target response using time gating. Assume that at the k th iteration, we reconstruct an image $\hat{\mathbf{x}}_{\text{res},k}$ using residual data $\{\mathbf{y}_{\text{res},k-1}^{(d,n)}\}$. With the target location, the residual signal is gated in time as

$$\hat{y}_{i_k}^{(d,n)}(t) = \begin{cases} y_{\text{res},k-1}^{(d,n)}(t), & |t - \tau_{i_k}^{(d,n)}| \leq \frac{20\lambda}{c} \\ 0, & |t - \tau_{i_k}^{(d,n)}| > \frac{20\lambda}{c} \end{cases}, \quad (15)$$

where $y_{\text{res},k-1}^{(d,n)}(t)$ is the time-domain residual signal, and $\tau_{i_k}^{(d,n)} = (\|\mathbf{r}_{d_0,n} - \mathbf{l}_{i_k}\| + \|\mathbf{r}_{d,n} - \mathbf{l}_{i_k}\|)/c$. Note that the time-gating boundary $(20\lambda)/c$ is determined by the maximum position perturbation. It can be tightened by considering the smooth trajectory of each radar platform. Let $\hat{y}_{i_k}^{\text{ref}}(t)$ be the time domain signal of the dominant vector ϕ_{i_k} of \mathbf{E}_{i_k} . We then take $\hat{y}_{i_k}^{\text{ref}}(t)$ as a reference, and estimate the time shift of $\hat{y}_{i_k}^{(d,n)}(t)$ in (15) as

$$\hat{\tau}_{\text{ref}}^{(d,n)} = \arg \max_{\tau} \left\{ \int \hat{y}_{i_k}^{(d,n)}(t) \cdot \hat{y}_{i_k}^{\text{ref}}(t + \tau) dt \right\}. \quad (16)$$

Let $\tilde{\tau}_{i_k}^{(d,n)} = (\|\tilde{\mathbf{r}}_{d_0,n} - \mathbf{l}_{i_k}\| + \|\tilde{\mathbf{r}}_{d,n} - \mathbf{l}_{i_k}\|)/c$ represent the unknown pulse propagation time from $\tilde{\mathbf{r}}_{d_0,n}$ to $\tilde{\mathbf{r}}_{d,n}$ via \mathbf{l}_{i_k} . Based on (16), and assuming the total propagation time is the same as that of the ideal distributed uniform array, we have the following equations to solve $\tilde{\tau}_{i_k}^{(d,n)}$ for all $d \in [1, 2, \dots, D]$ and $n \in [1, 2, \dots, N]$, such that the signals in (15) are coherent at \mathbf{l}_{i_k} after back-propagation,

$$\begin{cases} \tilde{\tau}_{i_k}^{(d,n)} - \tilde{\tau}_{i_k}^{\text{ref}} = \hat{\tau}_{\text{ref}}^{(d,n)}, \\ \sum_{n=1}^D \sum_{n=1}^N \tilde{\tau}_{i_k}^{(d,n)} = \sum_{n=1}^D \sum_{n=1}^N \tau_{i_k}^{(d,n)}. \end{cases} \quad (17)$$

With the solution $\tilde{\tau}_{i_k}^{(d,n)}$ of (17), $\tilde{\psi}_{i_k}^{(d,n)}$ is computed using (7).

C. Target signature extraction

Given $\tilde{\Psi}_{i_k}$, we determine \mathbf{E}_{i_k} using singular value decomposition (SVD) of $\tilde{\mathbf{Y}}_{\text{res},k} = \tilde{\mathbf{Y}}_{\text{res},k} \circ \tilde{\Psi}_{i_k}^*$ [16]:

$$\tilde{\mathbf{Y}}_{\text{res},k} = \mathbf{U}_k \Sigma_k \mathbf{V}_k^H, \quad (18)$$

where the superscript $*$ represents the phase conjugate and the superscript H represents the Hermitian transpose. Based on the SVD, we have

$$\mathbf{E}_{i_k} = \sigma_{k1} \mathbf{u}_{k1} \mathbf{v}_{k1}^H, \quad (19)$$

where σ_{k1} is the largest singular value of $\tilde{\mathbf{Y}}_{\text{res},k}$ representing the strength of the k th target, \mathbf{v}_{1,i_k}^H is the corresponding right singular vector representing the antenna pattern, and \mathbf{u}_{k1} is the corresponding left singular vector representing target signature,

$$\hat{\phi}_{i_k} = \mathbf{u}_{k1}. \quad (20)$$

Since the largest singular value σ_{1,i_k} is related to the target strength, we terminate our algorithm based on the target strength relative to the background noise. Specifically, we terminate when $\frac{\sigma_{k1} - \sigma_{k2}}{\sigma_{k1}} < \epsilon$ is satisfied, where σ_{k2} is the second largest singular value of $\tilde{\mathbf{Y}}_{\text{res},k}$, and ϵ is a threshold with value $0 < \epsilon < 1$.

D. Antenna position estimation

Based on the propagation time between each antenna and all k detected targets after the k th iteration, we estimate the array element positions by minimizing the cost functions

$$\begin{aligned} \hat{\mathbf{r}}_k^{(d_0,n)} = \arg \min_{\mathbf{r}} \left\{ \left| \left\langle \mathbf{r} - \mathbf{r}_{d_0,n}, \frac{\mathbf{r}_{d_0,n+1} - \mathbf{r}_{d_0,n}}{\|\mathbf{r}_{d_0,n+1} - \mathbf{r}_{d_0,n}\|} \right\rangle \right|^2 \right. \\ \left. + \sum_{k'=1}^k \frac{\sigma_{k'1}}{\sum_{k'=1}^k \sigma_{k'1}} \left(\|\mathbf{r} - \mathbf{l}_{i_{k'}}\| - \frac{\tilde{\tau}_{i_{k'}}^{(d_0,n)} c}{2} \right)^2 \right\}, \end{aligned} \quad (21)$$

and

$$\begin{aligned} \hat{\mathbf{r}}_k^{(d,n)} = \arg \min_{\mathbf{r}} \left\{ \left| \left\langle \mathbf{r} - \mathbf{r}_{d,n}, \frac{\mathbf{r}_{d,n+1} - \mathbf{r}_{d,n}}{\|\mathbf{r}_{d,n+1} - \mathbf{r}_{d,n}\|} \right\rangle \right|^2 \right. \\ \left. + \sum_{k'=1}^k \frac{\sigma_{k'1}}{\sum_{k'=1}^k \sigma_{k'1}} \left(\|\mathbf{r} - \mathbf{l}_{i_{k'}}\| - \left(\tilde{\tau}_{i_{k'}}^{(d,n)} - \frac{\tilde{\tau}_{i_{k'}}^{(d_0,n)}}{2} \right) c \right)^2 \right\}, \end{aligned} \quad (22)$$

for $d \neq d_0$. Each of the cost functions above is composed of two parts. The first part minimizes the azimuth discrepancy between the perturbed antenna and its ideal position. The second part restricts the distance in the range direction according to the propagation time. We use normalized target strength

$\sigma_{k'1}/(\sum_{k'=1}^k \sigma_{k'1})$ to weight the contribution of targets according to their scattering strength. While the cost functions in the optimization (21) and (22) are not convex, it might be possible to computationally find their global optimal solutions using the algorithm in [17] with a proper initial value of r . Note that since the antenna locations are determined based on distance measurements, which are translation and rotation invariant, we assume in our simulations that the mean and the dominant orientation of the perturbed array are the same as the ideal uniform array. To remove the translation and the rotation effects of the perturbed antennas and keep the distance between the perturbed antennas and targets unchanged, a linear transform on both the antenna locations and the target locations is necessary [18]. The updated antenna positions are then used to estimate the next target position using the residual data.

E. Image reconstruction

Given the estimated projection matrix

$$\hat{\mathbf{\Gamma}}_k^{(d,n)} = \left[\hat{\phi}_{i_1} \circ \tilde{\psi}_{i_1}^{(d,n)}, \hat{\phi}_{i_2} \circ \tilde{\psi}_{i_2}^{(d,n)}, \dots, \hat{\phi}_{i_k} \circ \tilde{\psi}_{i_k}^{(d,n)} \right], \quad (23)$$

scattering coefficients are computed using least squares,

$$\hat{\mathbf{x}}_k^{(d,n)} = (\hat{\mathbf{\Gamma}}_k^{(d,n)})^\dagger \hat{\mathbf{y}}^{(d,n)}, \quad (24)$$

where $\hat{\mathbf{x}}_k^{(d,n)}$ is a $k \times 1$ vector representing scattering coefficients of the k detected targets and the superscript \dagger denotes the Penrose-Moore pseudoinverse. A sparse image $\hat{\mathbf{x}}_{s,k}$ of the ROI is then reconstructed by assigning $\hat{\mathbf{x}}_k^{(d,n)}$ to the corresponding pixel locations as follows

$$\hat{\mathbf{x}}_{s,k}(i_{k'}) = \sum_{d=1}^D \sum_{n=1}^N \hat{\mathbf{x}}_k^{(d,n)}(k'), \quad (25)$$

for all $k' \in [1, \dots, k]$. For the purpose of target recognition, it is of great interest to preserve target signature information in imaging instead of just reconstructing sparse target phase centers. To this end, we first reconstruct data of an ideal side-looking uniform array using k detected target signature dictionaries [2] as follows

$$\hat{\mathbf{y}}_k^{(d,n)} = \sum_{k'=1}^k \hat{\mathbf{x}}_{i_{k'}}^{(d,n)} \cdot (\hat{\phi}_{i_{k'}} \circ \psi_{i_{k'}}^{(d,n)}), \quad (26)$$

where $\psi_{i_{k'}}^{(d,n)}$ has the same expression as $\tilde{\psi}_{i_{k'}}^{(d,n)}$ except using the ideal uniform element position $\mathbf{r}_{d,n}$. Based on the reconstructed data, we then perform delay-and-sum imaging to reconstruct a dense image

$$\hat{\mathbf{x}}_{d,k} = \sum_{d=1}^D \sum_{n=1}^N \left(\mathbf{\Psi}^{(d,n)} \right)^H \hat{\mathbf{y}}_k^{(d,n)}, \quad (27)$$

where $\mathbf{\Psi}^{(d,n)}$ is an $M \times I$ exponential matrix related to the ideal uniform array and the whole ROI.

IV. NUMERICAL SIMULATIONS

The simulation setup is depicted in Fig. 1. The ideal antenna positions of distributed arrays are indicated by black dots, and perturbed arrays by x-marks. Antenna positions are perturbed up to 10λ . A differential Gaussian pulse, illustrated in Fig. 2(a), is transmitted from the black array to illuminate

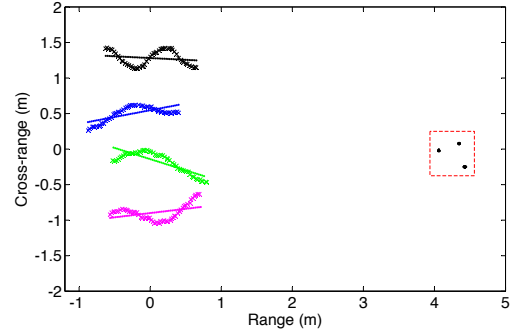


Fig. 1. Schematic representation of the distributed array imaging setup.

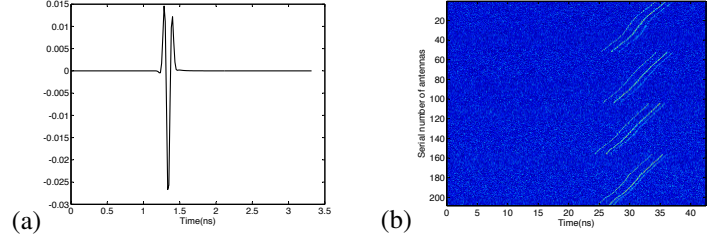


Fig. 2. (a) Emitted pulse and (b) Simulated noisy echoes received by four distributed arrays with PSNR=10dB.

the ROI. The received signals are simulated using the free-space Green's function and white Gaussian noise. Fig. 2(b) shows the simulated signal with PSNR = 10 dB.

In our algorithm, we set the total number of targets $K = 20$. The stop threshold is estimated using the signal PSNR as $\epsilon = (10^{\frac{0.5\text{PSNR}}{20}} - 1)/(10^{\frac{0.5\text{PSNR}}{20}})$. The imaging results are plotted in Fig. 3 with 30 dB dynamic range. In particular, Fig. 3(a) shows imaging using conventional delay-and-sum, ignoring unknown positions errors. Figure 3(b) shows imaging with initial phase-compensation using coherence analysis for a focus point at the center of the ROI. We can see that the image focus is better overall, but the three off-center targets are still not well focused. Instead, using our proposed approach, the sparse image is reconstructed using (25) as shown in Fig. 3(c). Each circle represents a sparse target, with the circle center corresponding to the target phase center and size proportional to the target scattering coefficient. A final dense image with target signatures using (27) is reconstructed in Fig. 3(d).

For comparison, we plot the result using the conventional delay-and-sum imaging method given the exactly perturbed position errors in Fig. 3(e); and the benchmark result of ideal uniform array in Fig. 3(f). We can notice that Figs. 3(e) and (f) are quite similar to each other since they both have known distributed array positions. However, due to the non-uniformly distributed array positions, both of the imaging results exhibit relative large sidelobes. For comparison, our imaging result in Fig. 3(d) presents much fewer sidelobes since the imaging result is based on reconstructed data of an ideal side-looking uniform array, which typically exhibits smaller sidelobes than a random array [19]. We verify our imaging algorithm on different noise data with PSNR = 10, 15, 20, and 30 dB. We plot the reconstructed dense image in Fig. 4(a) when PSNR = 20 dB, where we observe a clean and well-focused imaging result. We compare the relative reconstruction errors of different PSNRs in Fig. 4(b). Fig. 4 (b) shows that when

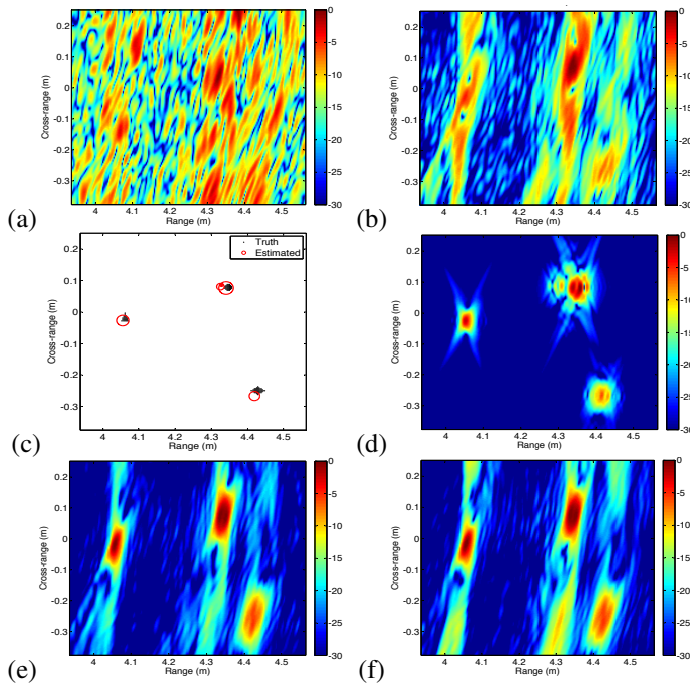


Fig. 3. Imaging results using simulated noisy data with different methods dealing with position errors: (a) delay-and-sum imaging with uniform array Green's function; (b) delay-and-sum imaging after initial phase compensation; (c) proposed CS based imaging with image-domain sparsity constraint; (d) proposed CS based imaging with targets' signatures; (e) delay-and-sum imaging with known position errors; (f) delay-and-sum imaging with ideal distributed uniform arrays.

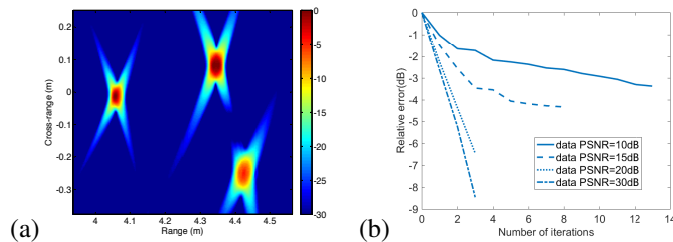


Fig. 4. (a) Reconstructed dense image with target signature using data of PSNR = 20 dB, (b) Relative reconstruction error of iterative autofocus algorithm.

the PSNR is high, we only need very few iterations to get a good reconstruction. With more noise we need more iterations to converge to a good reconstruction result.

V. CONCLUSIONS

We propose a data-driven method to perform automatic radar focused imaging. Our auto-focusing method is based on position error correction by exploiting data coherence and the spatial sparsity of the imaged area. Our method exhibits great advantages in dealing with antenna array with position errors up to several wavelengths of the radar center frequency, taking antenna radiation pattern and target signature into consideration. Imaging results with simulated noisy data demonstrate that our method significantly improved performance in imaging localized targets with only several iterations.

REFERENCES

- [1] C. R. Berger and J. M. F. Moura, "Noncoherent compressive sensing with application to distributed radar," in *2011 45th Annual Conference on Information Sciences and Systems (CISS)*, 2011.
- [2] D. Liu, U. Kamilov, and P. Boufounos, "Sparsity-driven distributed array imaging," in *IEEE International Workshop on Computational Advances in Multi-Sensor Adaptive Processing (CAMSAP)*, 2015.
- [3] D. E. Wahl, P. H. Eichel, D. C. Ghiglia, and C. V. Jakowatz Jr, "Phase gradient autofocus - a robust tool for high resolution SAR phase correction," *IEEE Trans. Aerospace and Electronic Systems*, vol. 30, no. 3, pp. 827–835, 1994.
- [4] X. Li, G. Liu, and J. Ni, "Autofocusing of ISAR images based on entropy minimization," *IEEE Trans. Aerospace and Electronic Systems*, vol. 35(4), pp. 1240–1252, October 1999.
- [5] W. Ye, T.S. Yeo, and Z. Bao, "Weighted least-squares estimation of phase errors for SAR/ISAR autofocus," *IEEE Trans. Geoscience and Remote Sensing*, vol. 37(5), pp. 2487–2494, September 1999.
- [6] F. Berizzi, M. Martorella, A. Cacciavano, and A. Capria, "A contrast-based algorithm for synthetic range-profile motion compensation," *IEEE Trans. Geoscience and Remote Sensing*, vol. 46(10), pp. 3053–3062, October 2008.
- [7] M. P. Nguyen and S. B. Ammar, "Second order motion compensation for squinted spotlight synthetic aperture radar," in *Asia-Pacific Conference on Synthetic Aperture Radar (APSAR)*, Sept 2013.
- [8] J. Yang, X. Huang, J. Thompson, T. Jin, and Z. Zhou, "Compressed sensing radar imaging with compensation of observation position error," *IEEE Trans. Geoscience and Remote Sensing*, vol. 52(8), pp. 4608–4620, August 2014.
- [9] X. Du, C. Duan, and W. Hu, "Sparsity representation based autofocusing technique for ISAR images," *IEEE Trans. Geoscience and Remote Sensing*, vol. 51(3), pp. 1826–1835, March 2013.
- [10] N. O. Onhon and M. Cetin, "A sparsity-driven approach for joint SAR imaging and phase error correction," *IEEE Trans. Image Processing*, vol. 21(4), pp. 2075–2088, April 2012.
- [11] D. Liu, "Sparsity-driven radar auto-focus imaging under over-wavelength position perturbations," in *The ninth IEEE Sensor Array and Multichannel Signal Processing Workshop*, 2016.
- [12] Y. Chi, L. L. Scharf, A. Pezeshki, and A. R. Calderbank, "Sensitivity to basis mismatch in compressed sensing," *IEEE Trans. Signal Processing*, vol. 59(5), pp. 2182–2195, May 2011.
- [13] Y. Tang, L. Chen, and Y. Gu, "On the performance bound of sparse estimation with sensing matrix perturbation," *IEEE Trans. Signal Processing*, vol. 61(17), pp. 4372–4386, September 2013.
- [14] D. Liu, G. Kang, L. Li, Y. Chen, S. Vasudevan, W. Joines, Q. Liu, J. Krolik, and L. Carin, "Electromagnetic time-reversal imaging of a target in a cluttered environment," *IEEE Trans. Antennas Propagat.*, vol. 53, pp. 3058–3066, Sept. 2005.
- [15] L. Meier S. van de Geer and P. Bühlmann, "The group lasso for logistic regression," *Journal of the Royal Statistical Society: Series B (Statistical Methodology)*, vol. 70, pp. 53–71, February 2008.
- [16] P. de Groen, "An introduction to total least squares," *Nieuw Archief voor Wiskunde*, vol. 14, pp. 237–253, July 1996.
- [17] A. Beck, P. Stoica, and J. Li, "Exact and approximate solutions of source localization problems," *IEEE trans. Signal Processing*, vol. 56(5), pp. 1770–1777, May 2008.
- [18] S. Umeyama, "Least-squares estimation of transformation parameters between two point patterns," *IEEE Trans. on Pattern Analysis and Machine Intelligence*, vol. 13, pp. 376–380, April 1991.
- [19] B. D. Steinberg, "The peak sidelobe of the phased array having randomly located elements," *IEEE Trans. Antennas and Propagation*, vol. 20(2), pp. 129–136, March 1972.